Available online at www.sciencedirect.com
ScienceDirect
International Journal of Heat and Mass Transfer 50 (2007) 4661–4667
International Journal of HEAT and MASS TRANSFER
www.elsevier.com/locate/ijhmt

A comparative study of the airside performance of heat sinks having pin fin configurations

Kai-Shing Yang [a], Wei-Hsin Chu [b], Ing-Yong Chen [b], Chi-Chuan Wang [a,*]

[a] *Energy and Environment Laboratories, Industrial Technology Research Institute, Bldg. 64, 195-6 Section 4, Chung Hsing Road, Chutung, Hsinchu 310, Taiwan*

[b] *Mechanical Engineering Department, National Yunlin University of Science and Technology, Yunlin 640, Taiwan*

Received 27 July 2006; received in revised form 7 March 2007
Available online 2 May 2007

Abstract

This study performs an experimental study of pin fin heat sinks having circular, elliptic, and square cross-section. A total of twelve pin fin heat sinks with inline and staggered arrangements were made and tested. The effect of fin density on the heat transfer performance is examined. For an inline arrangement, the circular pin fin shows an appreciable influence of fin density whereas no effect of fin density is seen for square fin geometry. This is associated with the unique deflection flow pattern accompanied with the inline circular fin configuration. For the staggered arrangement, the heat transfer coefficient increases with the rise of fin density for all the three configurations. The elliptic pin fin shows the lowest pressure drops. For the same surface area at a fixed pumping power, the elliptic pin fin possesses the smallest thermal resistance for the staggered arrangement.

Keywords: Pin fin; Plate fin; Heat sink

1. Introduction

Direct air-cooling is still the most popular means for cooling electronic products. Recognizing the poor heat transfer performance of air-cooling, secondary fin surface is usually exploited to solve the increased demand of heat dissipating. For further improvement of the overall heat transfer performance, augmentation via fin pattern is often employed. Among the fin configurations being implemented in practical applications, pin fin is regarded as one of the most effective heat transfer augmentation methods for providing boundary layer restarting and periodic vortex shedding. Notice that the pin fin is considered as the effective internal cooling means in the turbine blade, and the cooling of circuit boards. Extensive research for short pin arrays had been reported in the literature both numerically and experimentally [1–13]. The effects of length to diameter, array geometry, entrance length, and fin shape had been reported.

Note that the most common pin fin shape takes the form as cylindrical for its superior heat transfer performance. However, the corresponding pressure drop for cylindrical pin fin is also high. Hence there had been some contributions examining the different shapes of pin fin cross-section [7,13]. Chen et al. [7] conducted experiments associated with drop-shaped pin fins. They reported a slight enhancement of heat transfer coefficient with a remarkable 42–51% reduction of pressure drop. Recently, Sahiti et al. [13] numerically examined six kinds of pin shape, namely NACA, dropform, lancet, elliptic, circular, and square. Their simulation showed that NACA profile offers little advantage. Encompassing the constraints of same hydraulic diameter, coverage ratio, and pin length, circular pin fin having inline arrangement still outperforms other configurations.

The aforementioned results provided some preliminary information about the performance of pin fin heat sinks

* Corresponding author. Tel.: +886 3 5916294; fax: +886 3 5829782.
E-mail address: ccwang@itri.org.tw (C.-C. Wang).

0017-9310/$ - see front matter © 2007 Elsevier Ltd. All rights reserved.
doi:10.1016/j.ijheatmasstransfer.2007.03.006

Nomenclature

A_b	base surface area
A_c	cross-section area of the fin being tested
A_f	fin surface area
A_0	total surface area
D	diameter of the circular pin fin
D_h	hydraulic diameter
F_S	fin spacing
h	average convective heat transfer coefficient
L	duct length
N	number of fins
R	thermal resistance
r	unit area base thermal resistance
Re_{Dh}	duct Reynolds number
P	periphery of the fin being tested
P_d	triangular pitch
P_l	longitudinal pitch
Pr	Prandtl number
P_t	transverse pitch
$\dot{Q}_{conv}$	convective heat transfer
$T_{a,in}$	inlet air temperature
$T_{a,out}$	outlet air temperature
T_w	the average surface temperature
V_{fr}	frontal velocity
x^+	inverse Graetz number

Greek symbols

ΔP	pressure drop
η	fin efficiency
η_0	surface efficiency
ΔT_{LM}	log mean average temperature

subject to the influence of cross-section. However, the information is still far from conclusive. In this regard, it is the purpose of this study to present some quantitative data for pin fin having cylindrical, square, and elliptic configurations.

2. Experimental apparatus

The experiment apparatus is based on ASHRAE wind tunnel setup that is capable of measuring the heat transfer and pressure drop characteristics of the heat sinks. Two mains parts of the experimental apparatus are described below.

As seen in Fig. 1, experiments were performed in an open type wind tunnel. The ambient air-flow is driven to flow across the test section by a centrifugal fan regulated with an inverter. To avoid and minimize the effect of flow maldistribution in the experiments, an air straightener-equalizer and a mixer were provided at the upstream and downstream of test section respectively. The mixer is consisted of two layers of stainless steel mesh whereas the straightener was placed at the entrance of test system. The detailed geometry of straightener and the location of the mixer are shown in Fig. 1. The inlet and the exit temperatures across the sample were measured by two T-type thermocouple meshes. The inlet and outlet meshes are

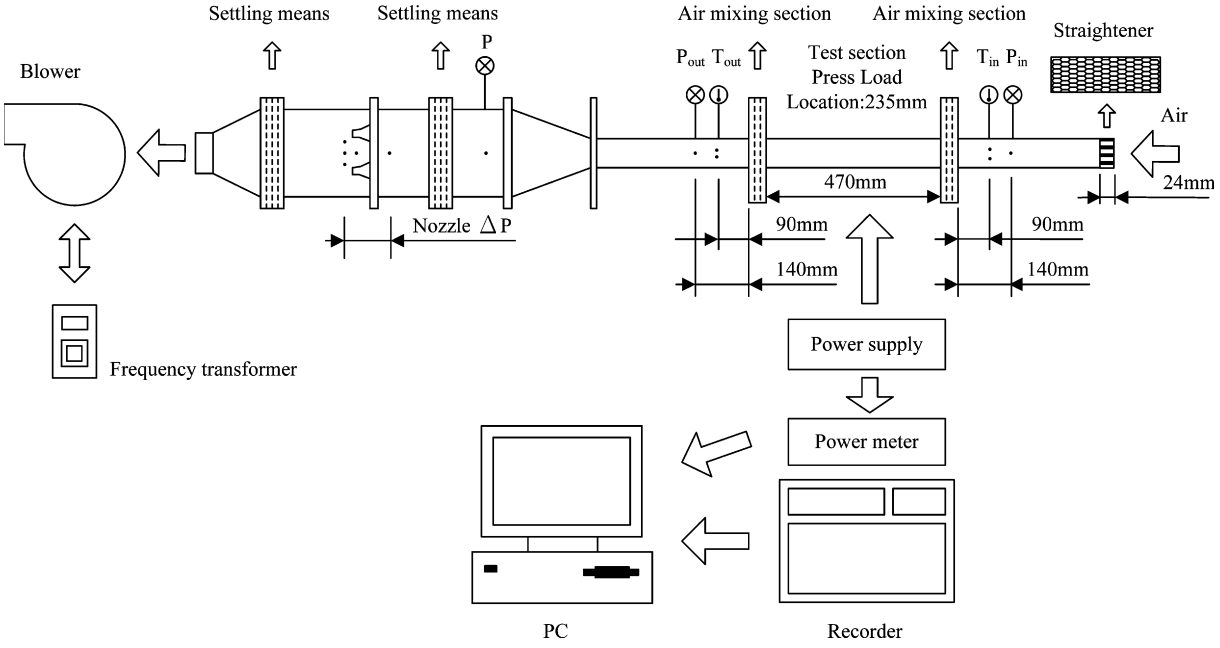

Fig. 1. Experimental set up.

placed outside the pressure taps to avoid influence on the measurements of pressure drops. The inlet measuring mesh consists of four thermocouples, while the outlet mesh contains eight thermocouples. The sensor locations inside the rectangular duct were established following ASHRAE [14] recommendation. These data signals were individually recorded and then averaged. The accuracies of the calibrated thermocouples are of 0.1 °C. During the isothermal test, variations of these thermocouples were within 0.2 °C. The pressure drop of the test sample and nozzle was detected by precision differential pressure transducer, reading to 0.1 Pa. The air-flow measuring station was a multiple nozzle code tester based on the ASHRAE 41.2 standard [15]. All the data signals are collected and converted by a data acquisition system (a hybrid recorder). The data acquisition system then transmitted the converted signals through Ethernet interface to the host computer for further operation.

A total of twelve pin fin heat sinks were made and tested, the corresponding fin patterns are circular, elliptic and square. The heat sinks were made from aluminum alloy with a thermal conductivity of 170 $W\,m^{-1}\,K^{-1}$. The geometries of heat sink are shown in Fig. 2, and their detailed dimensions are tabulated in Table 1. Note that the heat sinks are placed to fit the cross-section of the test duct through which no bypass occurs. For comparison purpose, two additional plate heat sinks were also made and tested. The base plates of the heat sinks are of square configuration with a length/width of 45 mm and a thickness of 2 mm. A film heater is attached to the bottom of heat sink. For measurement of the base temperature of heat sink, five thermocouples are installed beneath the base plate.

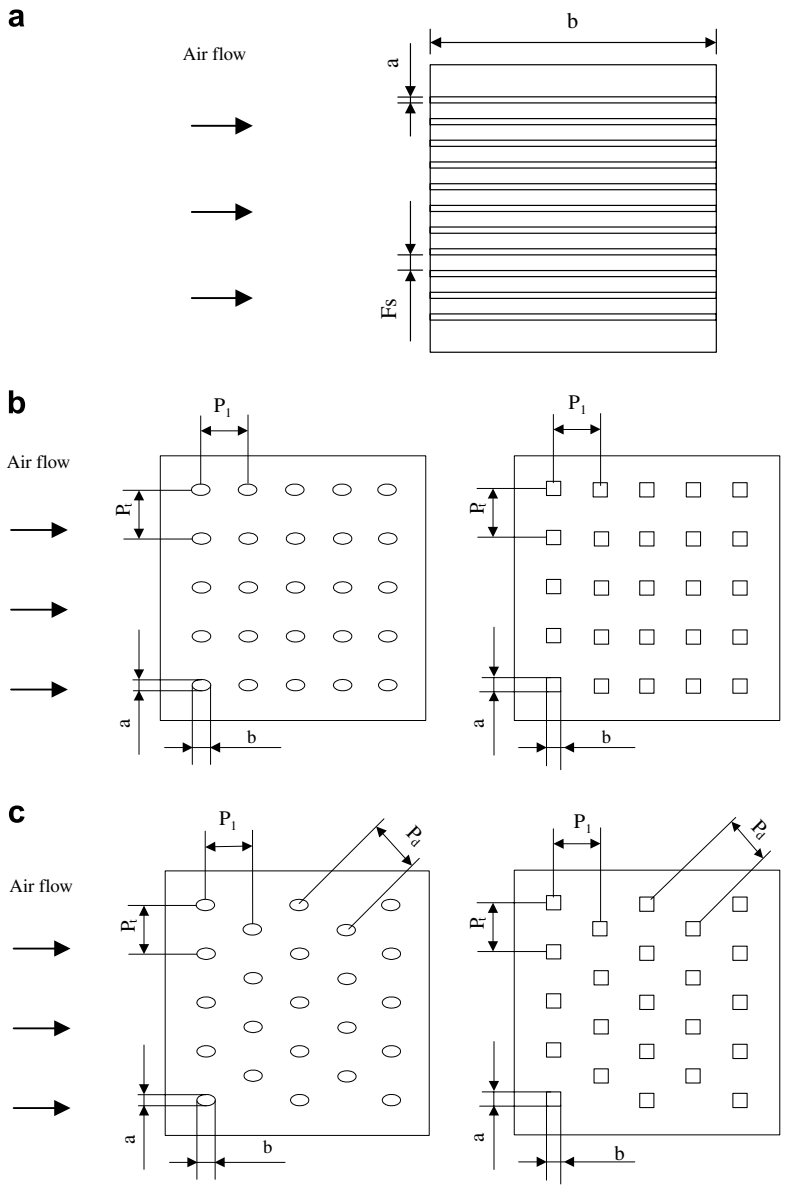

Fig. 2. Schematic of heat sinks geometry: (a) plate fin, (b) pin fin (inline) and (c) pin fin (staggered). The base plate of all test samples are 45 mm × 45 mm × 2 mm.

Table 1
Detailed geometry of the test heat sink (Unit: mm)

Sample no.	Type	Shape	a (mm)	b (mm)	N	P_t (mm)	P_l (mm)	P_d (mm)	F_S (mm)
	Plate								
#1		Plate	1	45	10	–	–	–	2.78
#2		Plate	1	45	15	–	–	–	1.43
	Pin fin								
#3	Inline	Elliptic	2	3	25	8.25	8	–	–
#4	Inline	Elliptic	2	3	49	5.5	5.33	–	–
#5	Inline	Square	2	2	25	8.25	8	–	–
#6	Inline	Square	2	2	49	5.5	5.33	–	–
#7	Inline	Circular	2	2	25	8.25	8	–	–
#8	Inline	Circular	2	2	49	5.5	5.33	–	–
#9	Staggered	Elliptic	2	3	25	11	5.34	7.67	–
#10	Staggered	Elliptic	2	3	41	8.25	4	5.75	–
#11	Staggered	Square	2	2	25	11	5.34	7.67	–
#12	Staggered	Square	2	2	41	8.25	4	5.75	–
#13	Staggered	Circular	2	2	25	11	5.34	7.67	–
#14	Staggered	Circular	2	2	41	8.25	4	5.75	–

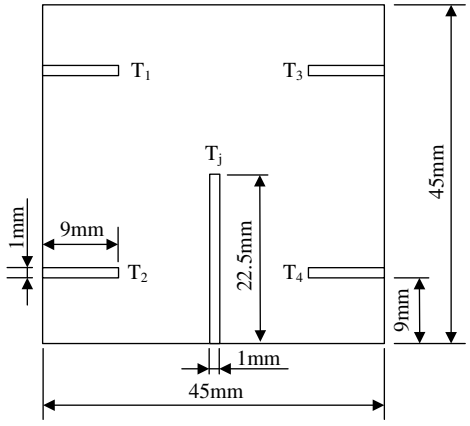

Fig. 3. Detailed locations of the thermocouples placed beneath the base plate.

Detailed locations of the thermocouples are shown in Fig. 3. During the tests, electric power supply provided 25 W power input to the heater. The bakelite board is installed beneath the film heater in order to minimizing the heat loss. The heat sinks were loaded to a constant force of 25 N throughout the experiment. This provided consistent thermal contact between the heat sinks and heater.

3. Analysis of heat sink

The average convection heat transfer coefficient is calculated as

$$h = \frac{\dot{Q}_{\text{conv}}}{A_0 \eta_0 \Delta T_{\text{LM}}} \tag{1}$$

where η_0 is the surface efficiency and ΔT_{LM} is the log mean average temperature of air at the test section. The surface efficiency may be written in terms of the fin efficiency, η, fin surface area A_f and total surface area A_0, i.e.

$$\eta_0 = 1 - \frac{A_f}{A_0}(1 - \eta) \tag{2}$$

where $A_0 = A_f + A_b$, A_f and A_b are the areas of the fin and base, respectively. The fin efficiency is given as

$$\eta_f = \frac{\tanh mL}{mL} \tag{3}$$

$$m = \sqrt{\frac{hP}{kA_c}} \tag{4}$$

where P denotes the periphery of the fin being tested and A_c represents the cross-section area of the fin. The fin efficiencies of the test samples, depending on the fin patterns, range from 0.85 to nearly unity.

The log mean temperature is given as

$$\Delta T_{\text{LM}} = \frac{(T_w - T_{a,\text{in}}) - (T_w - T_{a,\text{out}})}{\ln\left(\frac{T_w - T_{a,\text{in}}}{T_w - T_{a,\text{out}}}\right)} \tag{5}$$

Uncertainties in the reported experimental values of the heat transfer coefficients and pressure drops were estimated by the method suggested by Moffat [16]. The uncertainties range from 3.3 to 7.2% for h, and 2.6–11.2% for ΔP.

4. Results and discussion

Test results of pressure drop and heat transfer coefficient vs. frontal velocity for the test samples having inline and staggered arrangements are plotted in Figs. 4a and b, respectively. For the test pin fins, the major dimension ($a = 2$ mm, perpendicular to flow direction, shown in Fig. 2) is the same for all pin fin configurations. As expected, both heat transfer coefficient and the pressure drop increase with the rise of frontal velocity. For the increase of pressure drop among the test fin patterns, it can be found that the pressure drop increases considerably when the fin density is increased. However, the heat transfer characteristic subject to the influence of fin density is quite different among various fin configurations.

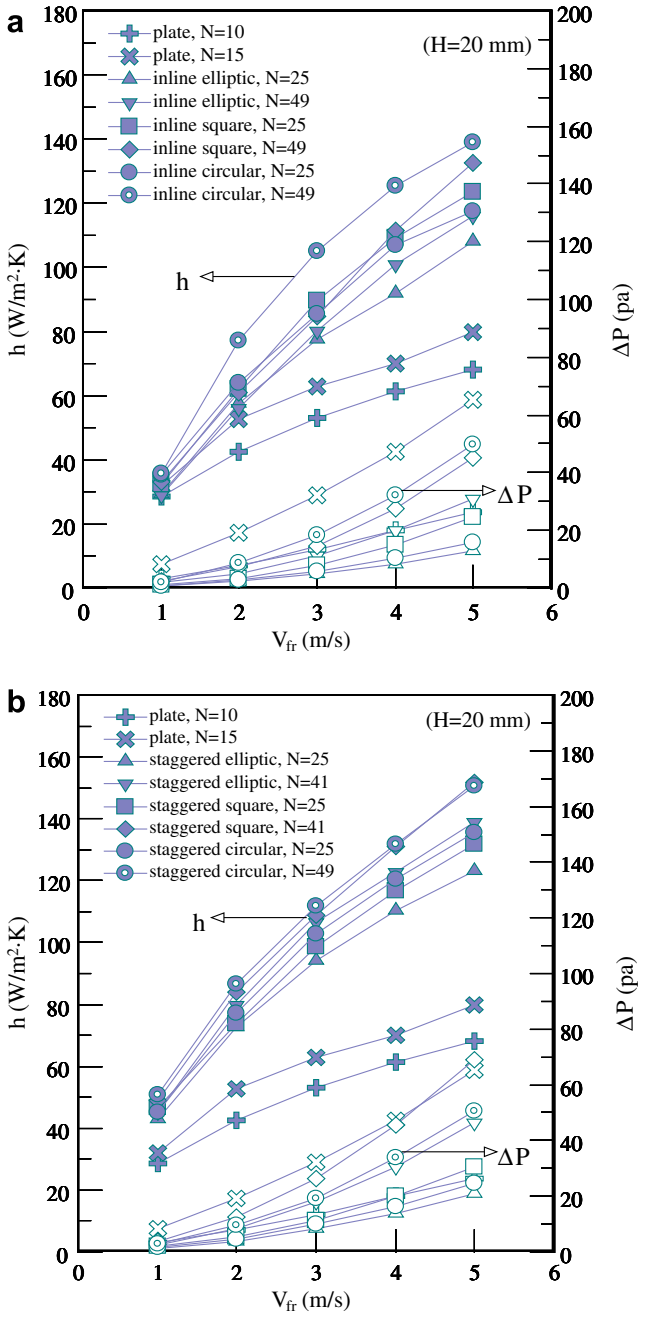

Fig. 4. Heat transfer coefficient and pressure drop vs. frontal velocity for plate fin and: (a) pin fin with an inline arrangement and (b) pin fin with a staggered arrangement.

For inline arrangement as shown in Fig. 4a, it is found that a considerable effect of fin density on the heat transfer coefficient of circular fin whereas the effect is small for an elliptic fin except when $V_{fr} > 3$ m/s. By contrast, a negligible influence of the fin density on the heat transfer performance is seen for the square pin fin. The results imply that there is a considerable difference of flow patterns among these pin configurations. For the circular tube configuration under inline arrangement, Ishigai and Nishikawa [17] examined the flow structure of gas flow in a single-column, single-row, and double-rows tube banks using the Schlieren photography technique. They reported that the Coanda effect may prevail when the gas flow penetrates across the tube gap. The tendency of fluids to follow a curved surface is known as the Coanda effect. For air-flow across the two adjacent tubes, the gap flow may direct to right or left which is known as a deflection flow. The existence of deflection flow may change the general vortex structure behind tubes, causing a better mixing and heat transfer performance. Ishigai and Nishikawa [17] reported that the deflection flow depends on the transverse and longitudinal ratios (P_t/D and P_l/D) and presented a map for identifying the existence of deflection flow. By carefully examining the location of the present circular pin fins with their map, it is found that it is unlikely for a loose fin density like sample #7 (Table 1) to have a deflection flow pattern whereas sample #8 is nearby the region to have a deflection flow pattern. Notice that the presence of deflection flow pattern prevents the formation of vortices, thereby causing a significant increase of heat transfer coefficient. As a consequence, one can see a considerable influence of fin density of the circular fin.

Opposite to the circular pin fin, the square pin fin possesses a non-curved surface in which the Coanda effect is much less prominent. Therefore, one can see that the effect of fin density is almost negligible. Analogously, the curvature variation of the elliptic pin fin is between the square and circular configuration, thus revealing only a very slight influence of fin density relative to that of the circular fin.

For the staggered arrangement, the heat transfer coefficients are all increased when the fin density is increased irrespective of the fin configuration. Apparently the presence of staggered arrangement had greatly altered the flow pattern. The subsequent row had forced the gap flow to be divided into two streams, thereby eliminating the special flow deflection characteristics. This can be evidently observed by typical flow visualization (e.g. Sparrow and Molki [18]). The results are in line with those of circular results summarized by Žukauskas [19]. The heat transfer performance of plate fin surface, either dense or loose fin pitch, is lower than those of pin fin surfaces, and the difference increases with the rise of frontal velocity. By examination of the applicable range of the inverse Graetz number ($x^+ = \frac{L/D_h}{Re_{Dh}Pr}$), it is found that the flow in the plate fin surface may fall within the fully developed region (i.e. $x^+ > 0.1$, [20]). Therefore, exploitation of interrupted surfaces like pin fin is rather effective.

For further comparison of the relative performance of the fin surfaces, Fig. 5 presents the thermal resistance to heat transfer for various pin configurations vs. supplied pumping power. For the same pumping power, the test results show that the thermal resistance for plate fin is the smallest among all the test surfaces. The results are in fact kind of misleading for the surface area of plate fin is significantly higher than those of pin fin surfaces. For pin fin configuration, the elliptic pin fin is the smallest for both inline and staggered arrangements. Part of the reasons is

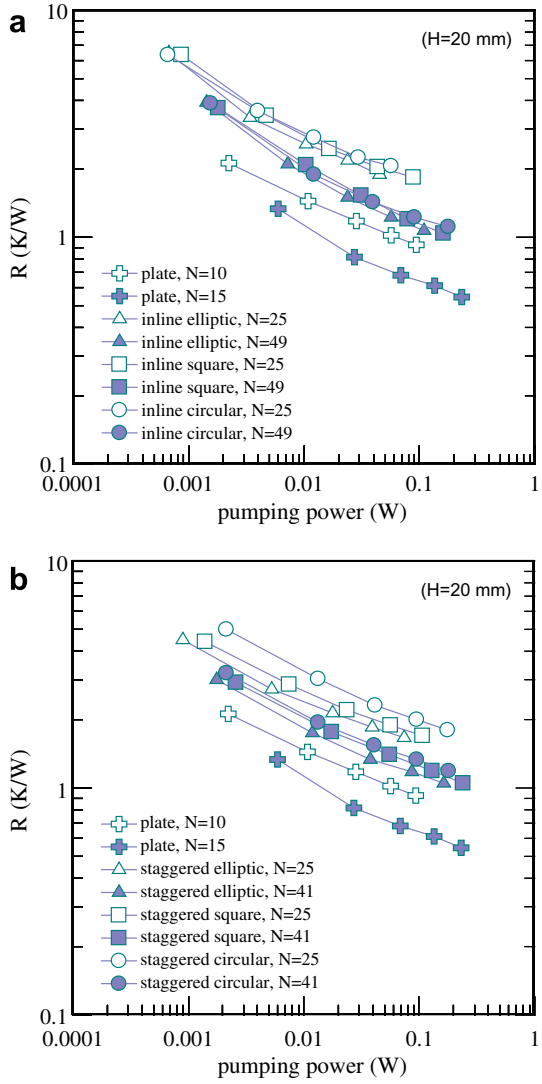

Fig. 5. Thermal resistances vs. pumping power of plate fin and: (a) pin fin with an inline arrangement and (b) pin fin with a staggered arrangement.

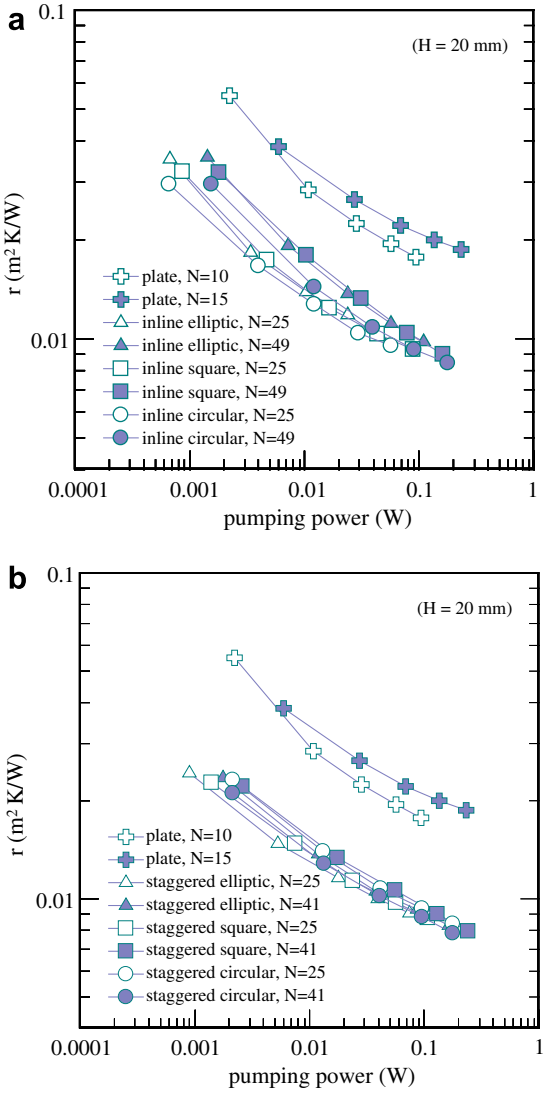

Fig. 6. Unit area base thermal resistances vs. pumping power of plate fin and (a) pin fin with an inline arrangement and (b) pin fin with a staggered arrangement.

attributed to the difference in surface area. Notice that the effective surface ratio among elliptic, square, and circular is roughly 1.45:1.25:1. Excluding the influence of surface area (equal surface area condition), it can be found that the circular pin fin possesses the smallest thermal resistance at a fixed pumping power and at an inline arrangement. One of the reasons for superior performance of the circular pin fin under inline arrangement is associated with the unique deflection flow. For further comparison of the test surfaces, the thermal resistances are normalized with unit area base (r, with unit of m^2 K W^{-1}) instead of the overall thermal resistance (R, with unit of K W^{-1}). Results of r vs. pumping power are shown in Fig. 6. In this diagram, one can clearly see that the plate fin holds the largest thermal resistance at a fixed pumping power. For the same pumping power, it is found that the inline arrangement circular yields the best performance, yet the elliptic pin fin slightly outperforms other pin fin geometry under staggered arrangement.

5. Conclusions

This study conducts a comparative study of pin fin heat sinks having circular, elliptic, and square cross-section. A total of twelve pin fin heat sinks having inline and staggered arrangements were made and tested. The effect of fin density on the heat transfer performance is examined. For an inline arrangement, circular pin fin shows an appreciable influence of fin density whereas virtually no effect of fin density is seen for square fin geometry. This is associated with the unique deflection flow pattern accompanied with the inline circular configuration. For the staggered arrangement, the heat transfer coefficient increases with the rise of fin density for all the three configurations. The elliptic pin fin shows the lowest pressure drops. For the same surface area and at a fixed pumping power, the circular pin fin possesses the smallest thermal resistance at an inline arrangement. One of the reasons for superior

performance of circular pin fin under inline arrangement is associated with the unique deflection flow. For a staggered arrangement where deflection flow pattern vanishes, the elliptic pin fin yields slightly better performance than circular pin fin surface.

Acknowledgements

The authors express gratitude for the supporting funding from the Department of Industrial Technology, Ministry of Economic Affairs, Taiwan.

References

[1] J. Armstrong, D. Winstanley, A review of staggered array pin fin heat transfer for turbine cooling applications, J. Turbomach. 110 (1988) 94–103.
[2] F.E. Ames, L.A. Dvorak, M.J. Morrow, Turbulent augmentation of internal convection over pins in staggered-pin fin arrays, J. Turbomach. 127 (2005) 183–190.
[3] F.E. Ames, L.A. Dvorak, Turbulent transport in pin fin arrays: experimental data and predictions, J. Turbomach. 127 (2006) 71–81.
[4] E.M. Sparrow, E.D. Larson, Heat transfer from pin-fins situated in an oncoming longitudinal flow which turns to cross-flow, Int. J. Heat Mass Transfer 25 (1982) 603–614.
[5] R.F. Babus'Haq, K. Akintunde, S.D. Probert, Thermal performance of a pin fin assembly, Int. J. Heat Fluid Flow 16 (1995) 50–55.
[6] R.A. Wirtz, R. Sohal, H. Wang, Thermal performance of pin fin fan-sink assemblies, J. Electron. Pack. 119 (1997) 26–31.
[7] Z. Chen, Q. Li, D. Meier, H.J. Warnecke, Convective heat transfer and pressure loss in rectangular ducts with drop-shaped pin fins, Heat Mass Transfer 33 (1997) 219–224.
[8] K. Al-Jamal, H. Khashasneh, Experimental investigation in heat transfer of triangular and pin fin arrays, Heat Mass Transfer 34 (1998) 159–162.
[9] M. Tahat, Z.H. Kodah, B.A. Jarrah, S.D. Probert, Heat transfer from pin fin arrays experiencing forced convection, Appl. Energ. 67 (2000) 419–442.
[10] N. Zheng, R.A. Wirtz, Cylindrical pin fin fan-sink heat transfer and pressure drop correlations, IEEE Trans. Compon. Pack. Technol. 25 (2002) 15–22.
[11] O.N. Şara, Performance analysis of rectangular ducts with staggered square pin fins, Energ. Convers. Manage. 44 (2003) 1787–1803.
[12] A. Horvat, B. Mavko, Hierachic modeling of heat transfer processes in heat exchangers, Int. J. Heat Mass Transfer 48 (2005) 361–371.
[13] N. Sahiti, A. Lemouedda, D. Stojkovic, F. Durst, E. Franz, Performance comparison of pin fin in-duct flow arrays with various pin cross-sections, Appl. Therm. Eng. 26 (2006) 1176–1192.
[14] ASHRAE Handbook Fundamental. SI-Edition, American Society of Heating, Refrigerating and air-conditioning Engineers, Inc., Atlanta, 1993, pp. 13.14–13.15.
[15] ASHRAE Standard 41.2-1987, Standard Methods for Laboratory Air-flow Measurement, American Society of Heating, Refrigerating and Air-Conditioning Engineers, Inc., Atlanta, 1987.
[16] R.J. Moffat, Describing the uncertainties in experimental results, Exp. Therm. Fluid Sci. 1 (1988) 3–17.
[17] S. Ishigai, E. Nishikawa, Experimental study of structure of gas flow in tube banks with tube axes normal to flow Part II; on the structure of gas flow in single-column, single-row, and double-rows tube banks, Bull. JSME 18 (1975) 528–535.
[18] E. M Sparrow, M. Molki, Effect of a missing cylinder on heat transfer and fluid flow in an array of cylinders in cross-flow, Int. J. Heat Mass Transfer 25 (1982) 449–456.
[19] A. Zukauskas, Heat transfer from tubes in cross-flow, Adv. Heat Transfer 8 (1972) 93–160.
[20] J.E. Sergent, A. Krum, Thermal Management Handbook for Electronic Assemblies, McGraw-Hill, New York, 1998.